

Original Research

# An Influence of Pyrite Oxidation on Generation of Unique Acidic Pit Water: A Case Study, Podwiśniówka Quarry, Holy Cross Mountains (South-Central Poland)

Z. M. Migaszewski<sup>1\*</sup>, A. Gałuszka<sup>1</sup>, P. Paślawski<sup>2</sup>, E. Starnawska<sup>3</sup>

<sup>1</sup>Pedagogical University, Institute of Chemistry, Geochemistry and the Environment Div.,  
5 Chęcińska St., 25-020 Kielce, Poland

<sup>2</sup>Central Chemical Laboratory, Polish Geological Institute, 4 Rakowiecka St., 00-975 Warsaw, Poland

<sup>3</sup>Electron Microscope Laboratory, Polish Geological Institute, 4 Rakowiecka St., 00-975 Warsaw, Poland

Received: July 14, 2006

Accepted: January 4, 2007

## Abstract

This report presents an assessment of pyrite weathering on the chemistry of water in the abandoned Podwiśniówka quarry of the Holy Cross Mountains (south-central Poland). This quarry did not operate for ore minerals, but for quartzites. The area of the pit pond enlarges each year generally as a result of an influx of spring snowmelt or heavy rainfall. The water examined reveals a very low pH, varying from 2.27 to 3.57 (with geometric mean value of 2.90), and unusual low concentrations of cations and anions, especially total Fe (2.7–24.0 mg·L<sup>-1</sup>) and SO<sub>4</sub><sup>2-</sup> (55–285 mg·L<sup>-1</sup>). With regard to its chemistry, this pond is unique compared to similar sites in Poland and even throughout the world. The low pH and element concentrations are attributed to the specific mineralogy of ore and gangue minerals, as well as complex bacterially catalyzed geochemical processes that have encompassed pyrite oxidation and iron oxidation/hydrolysis reactions.

**Keywords:** host rocks, ore and gangue minerals, pyrite oxidation, acid water chemistry, Podwiśniówka quarry, Holy Cross Mountains, south-central Poland

## Introduction

Microbial oxidation of pyrite (FeS<sub>2</sub>) and iron-bearing sulfides by oxygenized water generates acidic water, revealing a pH generally in the range of about 2 to 4. The process of releasing hydrogen ions triggers a chain of reactions that affect associating metal-sulfide and gangue minerals. Heavy metals can also be leached from host rocks that come into contact with sulfuric acid. In general, the low pH is always accompanied by high concentrations of

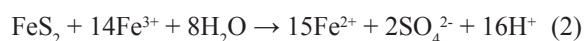
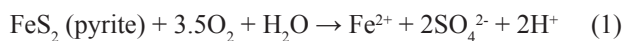
sulfates and heavy metals, varying from hundreds of milligrams to hundreds of grams per liter. The extremely acidic water (pH = -3.6), exhibiting simultaneously the highest sulfate and metal concentrations (about 760 and 200 g·L<sup>-1</sup>, respectively), was recorded in the inoperative Richmond Mine of Iron Mountain, northern California [1-3]. Of the sulfide minerals, pyrite is ubiquitous, occurring in nearly all polymetallic mineral deposits and many of the mineralized rock formations. The process of pyrite oxidation is often accentuated and accelerated by human activity, *i.e.* mining and construction works. Mine workings, mineral tailings and ponds, and artificial exposures of rock formations, containing scattered pyrite and other sulfide miner-

---

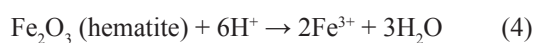
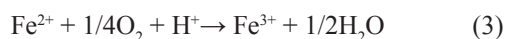
\*Corresponding author; e-mail: zmig@pu.kielce.pl

als, are potential pollution sources. Heavy-metal-bearing acid mine/rock waters have jeopardized the environment of many areas throughout the world [e.g. 1-8].

The pyrite can undergo oxidation by two natural oxidants, *i.e.* oxygen and even more effective ferric ( $\text{Fe}^{3+}$ ) iron [e.g. 2, 9-12], according to simplified reactions such as:



These two reactions bring about a considerable decrease in pH and an increase in concentrations of ferrous ( $\text{Fe}^{2+}$ ) and sulfate ions in water. The oxidation of pyrite (1) seems to be initiated by oxygen at pH about 6 because of the low solubility of ferric ( $\text{Fe}^{3+}$ ) iron at about neutral pH values. As a result of this reaction, the pH considerably decreases triggering the subsequent reaction (2), which can be 2–3 times orders of magnitude faster than the oxidation with oxygen and gives 8 times more hydrogen ions (but the same amount of sulfate ions).  $\text{Fe}^{3+}$  is derived from both oxidation of  $\text{Fe}^{2+}$  and partial dissolution of hematite/goethite, as indicated by the following theoretical reactions:



The reaction (4) consumes 6 times more hydrogen ions than the reaction (3), and does not seem to be predominant. Subsequently, the dissolved  $\text{Fe}^{3+}$  continues to hydrolyze and ferric hydroxide precipitates according to the reaction:



The reactions described above appear to be more complex. The oxidation of pyrite may occur on the pyrite-grain surface as a result of oxygen adsorption, and subsequently through colonization by chemolithotrophic acidophilic oxidizing bacteria, for example, *Acidithiobacillus ferrooxidans* or *A. thiooxidans*. These microorganisms also catalyze all the stages of pyrite oxidation with oxygen and subsequently ferric ions as the oxidants [e.g. 13, 14], increasing reaction rates by several orders of magnitude [15].

There are a variety of options for the prevention and remediation of acid-rock drainage. The main preventative and remedial measures encompass: no action, isolation of pyrite and iron-bearing sulfide outcrops or wastes from atmospheric oxygen and oxygenated waters (air sealing, partial or complete capping of the pyrite zone or dumps to prevent infiltration, surface-water diversion, ground-water interception, mine plugging), application of bactericides to sulfide-generating mine waters, lime neutralization, on-site leaching and solution extraction, or combined alternatives [e.g. 2, 14, 16-19].

One of the most interesting examples of the influence of mining activity on the environment is an acidic water pond located in the abandoned Podwiśniówka quarry (Fig. 1). It quarried only for quartzites and quartzitic sandstones. Exploratory works conducted two decades ago exposed a pyrite zone that quickly became a natural pollution source to open pit water, soil and biota. Acidic mine waters from some areas of Poland, *i.e.* the Sudetes and the Upper Silesia Coal Basin, have also been analyzed for pH and heavy metals [e.g. 20, 21]. However, none of these studies have recorded such a low pH and simultaneously low concentrations of sulfates, iron and other heavy metals. In general, the concentrations of sulfates and iron in acid mine waters are several to about ten times lower compared to those from Poland and many localities worldwide.

This report presents the results of pH and element determinations of this water, as well as chemical analyses of water sediment, pyrite, clayey shale and bentonite (altered tuff with prevailing clay minerals) performed during March 2004 through June 2006. The scope of this preliminary study also encompassed X-ray diffraction and SEM (combined with EDS system) examinations on some of the solid samples mentioned above. The principal objective was to explain the surprisingly low pH and element concentrations in the water examined. Based on the results derived from chemical determinations, the saturation indices for identified minerals were calculated using PHREEQC program for Windows [22, 23]. The results obtained in this study will serve as a reference level for comparison with future monitoring activities in the neighboring areas intended to record fluctuations in the distribution pattern of pH and elements.

## Materials and Methods

### Study Area Location and Characterization

The abandoned Podwiśniówka quarry is located in the westernmost part of the Main Range of the Holy Cross Mountains. This is part of a larger mining area composed of three separated quarries: the central operative (Wiśniówka Duża), and the western (Wiśniówka Mała) and eastern (Podwiśniówka) inoperative, occupying an area of several square kilometers (Fig. 1). These quarries do not quarry for ore minerals. Only quartzites and quartzitic sandstones have been quarried for manufacturing road aggregates and refractories. The geologic setting of this area is highly complex; all three quarries are located within a frontal folded, faulted and sliced zone of the Łysogóry Thrust composed of Middle and Upper Cambrian quartzites and quartzitic sandstones with numerous quartzitic siltstone, clayey shale, and subordinate tuff and bentonite interbeds [e.g. 24-27]. The Podwiśniówka quarry takes up an area of about 300×300 m.

On the western wall three rock series (tectonic slices) are exposed (Fig. 2A). In southern part of this section,

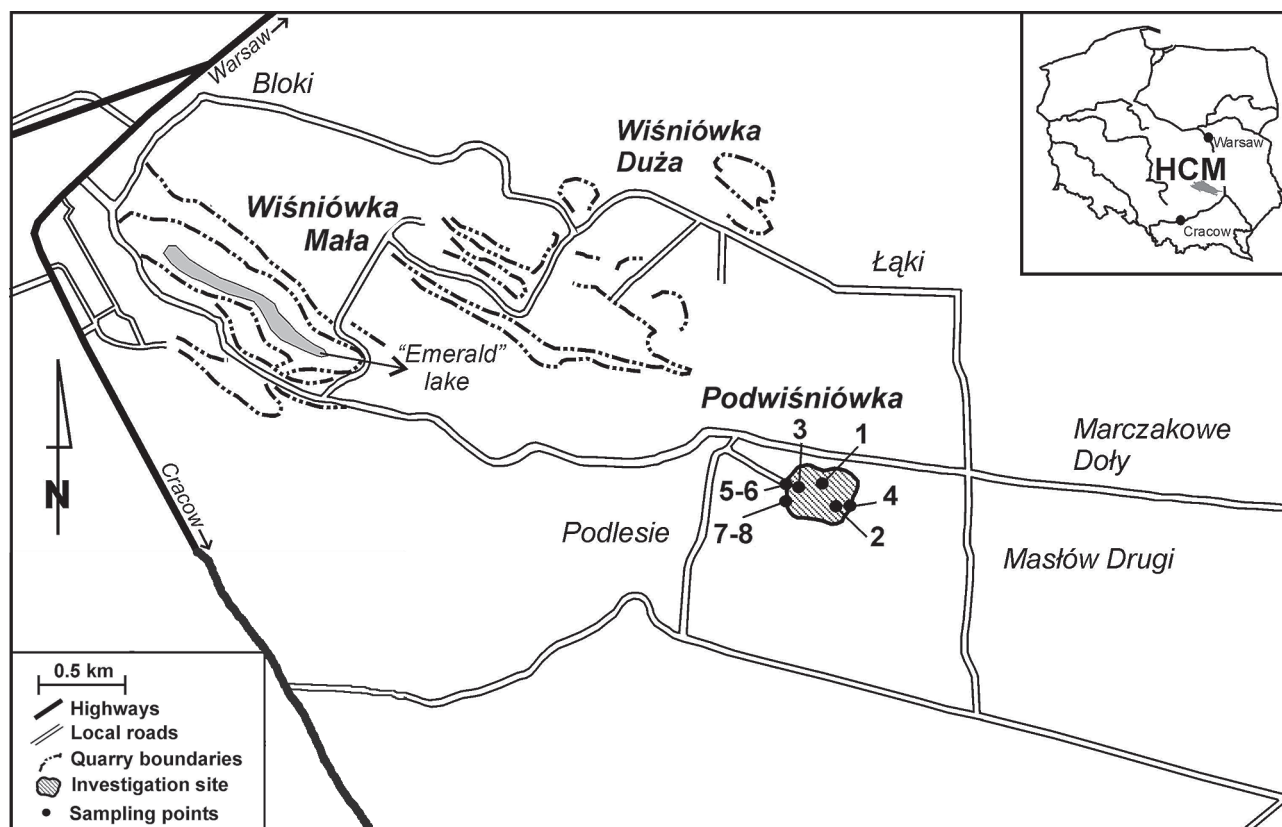


Fig. 1. Localization of the Podwiśniówka quarry with sampling points.

light gray fine-bedded quartzites with numerous tuff and bentonite interbeds crop out. These rocks do not contain scattered or veined pyrite, goethite and hematite. The towering central part of the section consists of gray medium-bedded quartzites with subordinate carbonaceous clayey shale interbeds reaching 1.5 m in thickness (Fig. 2B). These quartzites contain chlorite and goethite efflorescences on joint and fracture planes. In addition, some of these quartzites are densely cut by pyrite-quartz veinlets, locally passing into tectonic breccias composed of quartzite fragments cemented by fine-grained quartz and micro- to fine-grained pyrite (Fig. 2C and D). The biggest pyrite grains (reaching 0.5 mm in diameter) disclose a distinctive bronze tint, which is indicative of arsenic isomorphic admixtures [28]. In places, pyrite-quartz veinlets are covered with pale green grape-like variscite  $Al[PO_4] \cdot 2H_2O$ . At least some of the carbonaceous clayey shales also contain scattered pyrite grains and secondary goethite accumulations. The pyrite weathers rapidly and the mud-like oxidation products with associating gangue minerals are washed away by rainwater or meltwater into the pit. These two rock series dip northward at different angles (Fig. 2A and B). In contrast, the third (northern) part of this section consists of light gray to white nonbedded quartzites densely cut by quartz veins, locally passing into quartzitic-quartz breccias. The quartz veins are associated with hematite and goethite accumulations. These iron minerals impart rusty color to this tectonically disturbed and hydrothermally metamorphosed quartzite series. No significant pyrite accumulations have been recorded here.

These three series, *i.e.* tuff-bearing, pyrite-quartz, and hematite/goethite, extend eastward through the pit floor to the opposite low-lying wall. No detailed studies of pyrite and hematite/goethite mineralization have been conducted so far. Due to the strong tectonic deformations, it is not possible to detect a relationship between these two types of ore mineralizations.

The bottom of the open pit is partly filled in by a water pond whose surface varies depending on precipitation. During the spring snowmelt most of the pit is filled in by water, reaching at least 150×80 m in area and 1.5 m in depth. On the verge of the eastern wall, about 10 m above the pit floor, there is a small pond of 15×5 m in area, which can serve as a reference level to pit pond water chemistry. This small pond is located outside the pyrite zone within the tuff-bearing series, and its chemistry is influenced primarily by precipitation.

### Fieldwork and Sampling

Fieldwork was performed from March of 2004 through June of 2006. Except for geologic investigations, this included direct measurements of pH, conductivity (EC), redox potential (Eh) and temperature of water, using a pH-meter CP-103, an EC-meter CC-101, and a pH/Eh-meter CP-401 Elmetron, Poland. In addition, alkalinity and concentrations of  $Fe^{2+}$ ,  $Fe$  (total) and sulfates were determined using a field spectrophotometer LF-205 Slanidi, Poland.  $Fe^{3+}$  was computed as the difference between

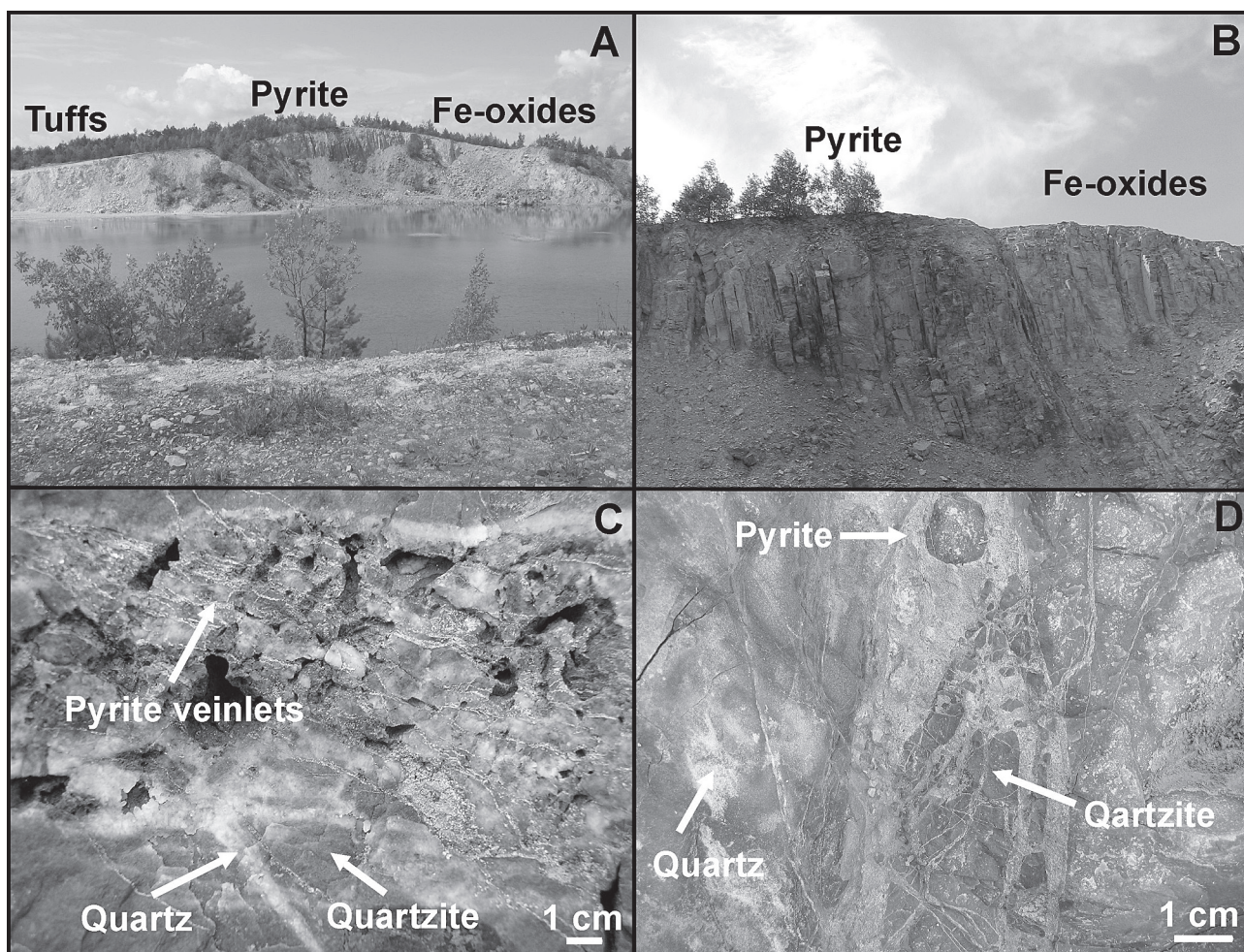


Fig. 2. (A) A view of the western wall of the Podwiśniówka quarry with a quartzite-carbonaceous clayey shale series containing quartz-pyrite mineralization (central photo side), a quartzite series with numerous tuff and bentonite interbeds in southern part (left photo side) and a tectonically brecciated quartzite series with hematite/goethite efflorescences on joint and fracture planes in northern part (right photo side). (B) A close-up of the central part. (C) (D) Quartz and pyrite veinlets cutting quartzite.

Fe (total) and  $\text{Fe}^{2+}$ . In all, 4 water and 2 sediment samples for complete chemical analyses were collected twice (May 25 and September 26 of 2004). One control water sample was also collected from the small pond. The water samples were collected prior to the sediment ones. Water samples for cation determinations were filtered with a  $0.2 \mu\text{m}$  filter. Sediment samples (weighing 100 g each) were collected in the western part of the pond close to the towering wall. Each individual sediment sample consisted of several to tens of *in-situ* sieved subsamples. The fraction which passed a 0.15-mm sieve was retained for chemical analysis [29]. The water samples were placed in plastic bottles and adequately preserved, while the sediment samples were placed in dark glass jars and chilled to about  $0^\circ\text{C}$ .

In addition, 4 duplicate pyrite, clayey shale, bentonite and soil samples of about 50–500 g were collected and preserved in plastic bags (for location of sampling points see Fig. 1). During sample collection and preparation, procedures were followed to minimize the possibility of contamination.

### Sample Preparation and Analysis

After drying at ambient temperature (about  $16^\circ\text{C}$ ), the sediment, clayey shale, bentonite and pyrite samples were disaggregated to pass a  $<0.063 \text{ mm}$  sieve using a Fritsch's blender. The powdered samples were then pelleted with wax (6 g sample and 1.5 g Merck wax).

The chemical analyses were performed according to methods and techniques used for geologic and environmental samples in the Central Chemical Laboratory of the Polish Geological Institute in Warsaw. Four samples were randomly selected for routine replicate analyses, and international standards, *i.e.* SRM 1643e; TMDA-54.3 (water), Lake Sediment LKSD-3, Stream Sediment STSD-1, Riverclay 921, were inserted accordingly.

The consecutive steps in the complete chemical analyses followed:

Water:

- (1) Unfiltered water samples were analyzed for anions using a high-performance liquid chromatograph (Waters HPLC Ion Chrom) with a conductometric detector (Br,

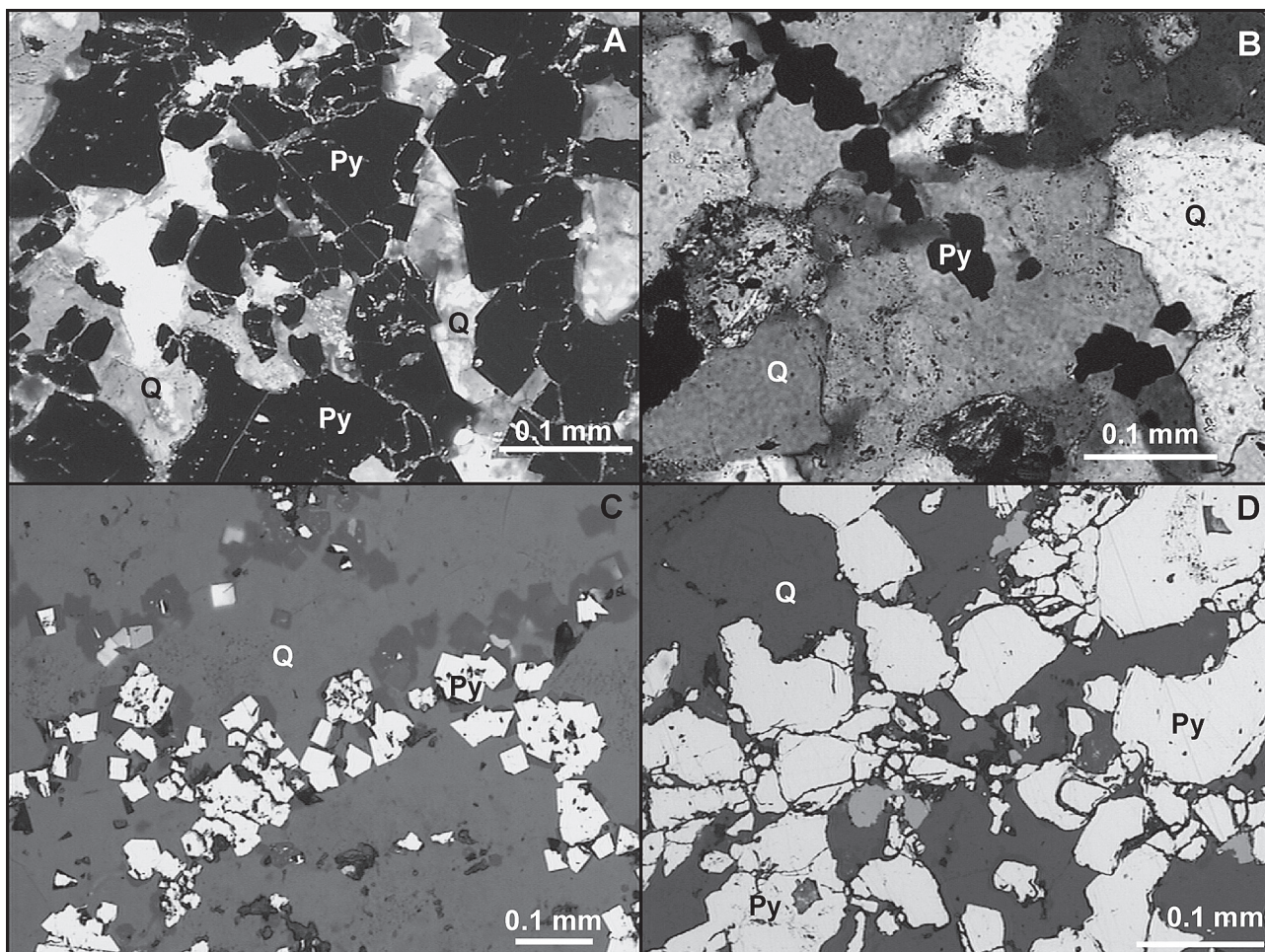


Fig. 3. Micrographs. (A) Pyrite aggregates in fine-grained quartz. Transmitted light, one nicol. (B) Pyrite grains in medium-grained quartz. Transmitted light, crossed nicols. (C) (D) Pyrite aggregates in quartz. Reflected light, one nicol.

Cl<sup>-</sup>, F<sup>-</sup>, HPO<sub>4</sub><sup>2-</sup>, SO<sub>4</sub><sup>2-</sup>) and a UV detector (NO<sub>2</sub><sup>-</sup>, NO<sub>3</sub><sup>-</sup>). NH<sub>4</sub><sup>+</sup> was determined using a spectrophotometer-UV-vis (Varian – model Cary-1e). Besides, HCO<sub>3</sub><sup>-</sup> was determined with a spectrophotometer LF-205 Slandi, Poland, whereas COD (chemical oxygen demand) using a spectrophotometer SPF Pastel UV Secomam.

(2) Filtered water samples were analyzed for 21 elements (Al, As, Ba, Ca, Cd, Co, Cr, Cu, Fe, K, Mg, Mn, Mo, Na, Ni, Pb, Si, Sr, Ti, V, Zn) using inductively coupled plasma-optical emission spectrometry (ICP-OES; multichannel spectrometer Jobin-Yvon – model PANORAMA with horizontal plasma). The total organic carbon (TOC) content of water was estimated using a spectrophotometer SPF Pastel UV Secomam.

Sediment, minerals, rocks:

For the purpose of this study the solid samples were analyzed for 22 elements (detection limits in parentheses), *i.e.* Al (50 mg·kg<sup>-1</sup>), As (3 mg·kg<sup>-1</sup>), Ba (10 mg·kg<sup>-1</sup>), Ca (50 mg·kg<sup>-1</sup>), Cd (3 mg·kg<sup>-1</sup>), Co (3 mg·kg<sup>-1</sup>), Cr (3 mg·kg<sup>-1</sup>), Cu (5 mg·kg<sup>-1</sup>), Fe (100 mg·kg<sup>-1</sup>), K (50 mg·kg<sup>-1</sup>), Mg (100 mg·kg<sup>-1</sup>), Mn (10 mg·kg<sup>-1</sup>), Mo (2 mg·kg<sup>-1</sup>), Na (100 mg·kg<sup>-1</sup>), Ni (5 mg·kg<sup>-1</sup>), Pb (3 mg·kg<sup>-1</sup>), S (50 mg·kg<sup>-1</sup>), Si (100

mg·kg<sup>-1</sup>), Sr (2 mg·kg<sup>-1</sup>), Ti (10 mg·kg<sup>-1</sup>), V (5 mg·kg<sup>-1</sup>) and Zn (2 mg·kg<sup>-1</sup>), using X-ray fluorescence spectrometry (XRF; spectrometer Philips PW 2400).

In addition, identification of mineral phases in pyrite, shale, soil and sediment samples was done with X-ray diffraction (XRD; diffractometer Philips X'Pert PW 3020) using K- $\alpha$  and K- $\beta$  wavelengths 1.54056 and 1.38222 Å. The XRD determinations were performed in the Central Chemical Laboratory of the Polish Geological Institute in Warsaw.

Ore and gangue minerals were examined petrographically using a polarized microscope Axilolab Carl Zeiss. The pyrite and ferric oxides and hydroxides were studied with a LEO 1430 (signal A = SE1, and BEI, magn. = 91–4240 $\times$ , EHT = 15.00 kV, WD = 21 mm) [Scanning Electron Microscopy (SEM) combined with EDS system] at the Electron Microscopy Laboratory of the Polish Geological Institute in Warsaw. Semi-quantitative chemical analyses of selected minerals were done with an EDS ISIS Detector (Oxford Instruments Ltd.). International standards, *i.e.* 30. Pyrite and 19. Skutterudite (SPI Standards 53 Minerals 02753-AB, West Chester, PA 19381-0656 USA), were used to lower the detection limit of As to 0.5%.

In addition, the saturation indices (SI) were calculated for identified minerals using the PHREEQC program for Windows [22, 23]. The saturation index is defined as:  $SI = \log(IAP/K_{sp})$ , where IAP is ion activity product and  $K_{sp}$  is the solubility product for a given temperature. This means that when  $IAP = K_{sp}$ , then  $SI = 0$  and water is at thermodynamic equilibrium with respect to the mineral. When  $SI > 0$ , water is supersaturated with respect to the mineral and this mineral should precipitate. In contrast, if  $SI < 0$ , water is undersaturated with respect to the mineral, this mineral should dissolve.

## Results

The results of field measurements of acidic pit water during March of 2004 through June of 2006 (including pH, EC, temperature, Eh, and concentrations of  $SO_4^{2-}$ ,  $Fe^{2+}$  and  $Fe^{3+}$ ) are presented in Table 1. The lowest pH (2.27, geometric mean 2.52) was recorded in March of 2005, whereas the highest one (3.57, mean 3.49) in May of 2006. The geometric mean pH value of the examined water for the whole study period was 2.90 ( $n = 76$ ). The pH dropped after thawing of thick snowpack loaded with pyrite oxidation products in April and May of 2004, March of 2005 and April of

Table 1. Geometric mean values of pH, conductivity (EC), redox potential (Eh), temperature (T) and concentrations of  $SO_4^{2-}$ ,  $Fe^{2+}$  and  $Fe^{3+}$  in the acidic pit pond water derived from field measurements.

Date of sampling	pH	EC $\mu S \cdot cm^{-1}$	Eh mV	T $^{\circ}C$	$SO_4^{2-}$	$Fe^{2+}$	$Fe^{3+}$
					mg·L <sup>-1</sup>		
March 25, 2004 (n = 5)	2.92	595	–	9.2	146	–	–
April 14, 2004 (n = 6)	2.71	585	–	14.0	–	–	–
May 25, 2004 (n = 4)	2.61	597	–	16.7	–	4.5*	1.6*
June 24, 2004 (n = 3)	3.06	671	485	24.2	157*	4.0*	2.0*
July 30, 2004 (n = 2)	3.26	601	–	23.7	–	–	–
August 31, 2004 (n = 2)	3.01	809	–	19.5	187	3.0	1.6
September 26, 2004 (n = 2)	3.13	630	–	16.0	285*	4.5*	8.5*
November 15, 2004 (n = 3)	2.58	598	–	3.2	–	–	–
December 4, 5, 2004 (n = 5)	2.80	426	–	2.8	195*	12.5*	3.0*
January 15, 2005 (n = 3)	2.92	702	–	2.4	230*	11.0*	13.0*
March 26, 2005 (n = 5)	2.52	341	–	9.9	–	–	–
April 7, 2005 (n = 3)	2.91	495	–	13.8	163	7.5	7.3
May 7, 2005 (n = 3)	3.06	484	–	14.5	93	2.9	6.2
June 4, 2005 (n = 3)	3.25	612	–	23.3	97	2.6	3.2
July 8, 2005 (n = 3)	3.18	680	–	28.5	114	2.0	1.3
August 5, 2005 (n = 3)	2.86	814	–	18.7	105	1.9	1.6
September 9, 2005 (n = 3)	2.83	863	–	24.8	119	2.8	0.4*
October 6, 2005 (n = 3)	2.99	747	–	18.8	156	2.4	0.9
November 14, 2005 (n = 3)	2.83	827	–	5.6	166	1.4	2.6
December 7, 2005 (n = 3)	2.87	526	–	8.7	169	1.9	0.0
April 1, 2006 (n = 3)	2.81	345	–	8.3	55	3.3	0.6
May 6, 2006 (n = 3)	3.49	895	–	18.8	152	2.3	12.1
June 12, 2006 (n = 3)	3.28	1018	–	23.8	143	4.5	4.6
$M_G$	2.90	616	–	11.9	131	3.0	2.6
	n = 76	n = 72	n = 3	n = 66	n = 43	n = 43	n = 43

NOTE: \*Determinations made on 1 sample only;  $Fe^{3+}$  computed as the difference between Fe (total) and  $Fe^{2+}$ ; uncertainty at 0.05 probability level is about 3% for pH, 5% for EC and Eh, and 10% for the remaining species.

Table 2. Geometric mean values of pH, conductivity (EC) and temperature (T) in the small pond water derived from field measurements.

Date of sampling	pH	EC $\mu\text{S}\cdot\text{cm}^{-1}$	T $^{\circ}\text{C}$
April 14, 2004	5.87	25	–
May 25, 2004	5.74	20	15.0
June 24, 2004	5.88	15	24.5
July 30, 2004	5.96	20	23.5
August 31, 2004	5.62	37	19.0
September 26, 2004	5.70	25	14.0
November 15, 2004	5.66	28	3.5
December 4, 5, 2004	5.39	27	1.0
January 15, 2005	5.42	36	2.0
March 26, 2005	5.03	23	3.0
June 4, 2005	6.06	25	24.5
July 8, 2005	6.19	11	26.5
August 5, 2005	4.84	21	18.0
September 9, 2005	5.68	12	21.0
June 4, 2005	4.87	31	9.0
June 12, 2006	6.26	21	22.0
$M_G$	5.65	22	10.6
	n = 16	n = 16	n = 15

2006. In addition, the lower pH was also recorded in November of 2004 after a drought that considerably decreased a pit pond area. The highest pH values were recorded in July of 2004, June of 2005 and May of 2006. In contrast, the pH of small pond water varied from 4.84 to 6.26 with geometric mean of 5.65 (Table 2).

The conductivity of acidic pit water varied from 291 (mean 345)  $\mu\text{S}\cdot\text{cm}^{-1}$  in April of 2006 through 1102 (mean 1018)  $\mu\text{S}\cdot\text{cm}^{-1}$  in June of 2006, with geometric mean value of 616  $\mu\text{S}\cdot\text{cm}^{-1}$  (n = 72). In contrast, the EC of small pond water varied from 11 in July of 2005 to 37  $\mu\text{S}\cdot\text{cm}^{-1}$  in August of 2004 with geometric mean value of 22  $\mu\text{S}\cdot\text{cm}^{-1}$  (n = 16) (Table 2).

The concentration of  $\text{SO}_4^{2-}$  in the acidic pit water was in the range of 55  $\text{mg}\cdot\text{L}^{-1}$  (April of 2006) to 285  $\text{mg}\cdot\text{L}^{-1}$  (September of 2004), with geometric mean value of 131  $\text{mg}\cdot\text{L}^{-1}$  (n = 43) (Tables 1 and 3). Alkalinity of this water never exceeded 0.1  $\text{mg}\cdot\text{L}^{-1}$   $\text{CaCO}_3$ . In contrast, the small pond water showed only trace levels of  $\text{SO}_4^{2-}$  (4  $\text{mg}\cdot\text{L}^{-1}$ ) and low alkalinity (3.5  $\text{mg}\cdot\text{L}^{-1}$   $\text{CaCO}_3$ ). The remaining anions occurred in the acidic pit water either in trace amounts ( $\text{Cl}^-$ ,  $\text{F}^-$ ,  $\text{NH}_4^+$ ,  $\text{NO}_3^-$ ) or below detection limits for a given analytical method ( $\text{Br}^-$ ,  $\text{NO}_2^-$ ,  $\text{HCO}_3^-$ ,  $\text{HPO}_4^{2-}$ ) (Table 3).

The redox potential (477–489 mV) indicates somewhat oxygenized conditions in the acidic pit water examined. This value was slightly higher than in the small pond water (329 mV). Compared to the small pond water, the acidic pit water showed much higher concentrations of cations, especially Al, Ca, As, Co, Cr, Cu, Fe, Mn, Ni

Table 3. Alkalinity and concentrations of ions in the pit pond and small pond waters of the Podwiśniówka quarry.

No.	Sampling points	Date of sampling	Alkalinity $\text{mg}\cdot\text{L}^{-1}$ $\text{CaCO}_3$	COD	$\text{HCO}_3^-$	TOC	$\text{Cl}^-$	$\text{F}^-$	$\text{NH}_4^+$	$\text{NO}_3^-$	$\text{SO}_4^{2-}$
				$\text{mg}\cdot\text{L}^{-1}$							
1.	Pit pond (1)	May 25, 2004	<0.1	12.3	<0.1	5.2	1.42	0.20	0.37	1.83	149
2.	Pit pond (2)	May 25, 2004	<0.1	12.1	<0.1	5.0	1.56	0.16	0.37	1.81	149
3.	Pit pond (3)	May 25, 2004	<0.1	12.1	<0.1	5.1	1.70	0.32	0.37	1.84	151
4.	Pit pond (3)	Sept. 26, 2004	<0.1	28.8	<0.1	11.1	1.73	<0.10	1.39	1.15	243
5.	Small pond (4)	May 25, 2004	3.5	20.2	4.3	7.7	0.93	<0.10	0.06	0.07	4

NOTE: COD – chemical oxygen demand;  $\text{Br}^-$  – <0.10  $\text{mg}\cdot\text{L}^{-1}$ ,  $\text{NO}_2^-$  – <0.01  $\text{mg}\cdot\text{L}^{-1}$ ,  $\text{HPO}_4^{2-}$  – <1.00  $\text{mg}\cdot\text{L}^{-1}$ . Uncertainty at 0.05 probability level is about 11% for TOC, and 10% for the remaining species. For location of sampling points (in parentheses) see Fig. 1

No.	Al	As	Ba	Ca	Cd	Co	Cr	Cu	Fe	K	Mg	Mn	Na	Ni	$\text{SiO}_2$	Sr	Ti	Zn
	$\mu\text{g}\cdot\text{L}^{-1}$																	
1.	4990	20	20	14000	1	45	14	152	6260	1300	2000	286	1300	50	4600	51	<2	82
2.	4940	20	20	13900	1	45	14	150	6270	1300	2000	289	1300	50	4600	51	<2	83
3.	4930	20	21	14000	1	45	14	150	6330	1500	2000	293	1300	51	4500	53	<2	86
4.	9170	60	16	22800	2	68	31	210	11750	2900	3500	471	2300	76	7400	79	2	173
5.	100	<10	9	2100	<1	<2	<3	<2	2600	1700	600	40	<500	<5	600	12	6	29

NOTE: Symbol < means below detection limit for a given element; Mo – <3  $\mu\text{g}\cdot\text{L}^{-1}$ , Pb – <10  $\mu\text{g}\cdot\text{L}^{-1}$ , V – <2  $\mu\text{g}\cdot\text{L}^{-1}$ . Uncertainty at 0.05 probability level is about 10%.

Table 4. Concentrations of selected elements in water sediment, pyrite, clayey shale, bentonite, soil (above tuff/bentonite zone).

Medium (sampling point)	Al <sub>2</sub> O <sub>3</sub>	CaO	Fe <sub>2</sub> O <sub>3</sub>	K <sub>2</sub> O	MgO	MnO	Na <sub>2</sub> O	S	SiO <sub>2</sub>	TiO <sub>2</sub>
	%									
Sediment (3)*	19.18	0.02	3.96	3.80	0.66	0.006	0.22	0.338	56.48	1.065
Sediment (3)**	20.87	0.04	6.88	4.27	0.72	0.007	0.36	0.711	59.05	1.163
Pyrite (5)	0.88	0.19	–	0.08	<0.01	0.003	<0.01	–	17.03	0.060
Shale (6)	12.35	0.04	5.36	2.71	0.33	0.008	0.16	2.352	35.10	1.304
Bentonite (7)	24.90	0.19	1.04	5.31	0.97	0.006	0.16	0.044	56.06	1.123
Soil (8)	11.32	0.16	2.67	2.04	0.59	0.022	0.66	<0.010	67.64	0.749

NOTE: For location of sampling points (in parentheses) see Fig. 1. Uncertainty at 0.05 probability level is 10%. \*Sampled on May 25, 2004, \*\*sampled on September 26, 2004

Medium (sampling point)	As	Ba	Cd	Co	Cr	Cu	Mo	Ni	Pb	Sr	V	Zn
	mg·kg <sup>-1</sup>											
Sediment (3)*	1067	877	5	<5	84	44	8	6	39	157	114	19
Sediment (3)**	1138	1044	<3	7	104	50	7	7	44	202	133	23
Pyrite (5)	9666	13	19	31	<3	123	4	186	26	24	10	16
Shale (6)	1484	428	<3	28	57	34	13	27	71	201	74	18
Bentonite (7)	13	409	<3	<3	132	12	5	11	11	147	130	18
Soil (8)	171	397	7	13	43	23	6	9	24	78	53	32

Symbol < means below detection limit for a given element. Uncertainty at 0.05 probability level is 10%

(Table 3). The mean geometric concentrations of Fe<sup>2+</sup> and Fe<sup>3+</sup> were 3.0 and 2.6 mg·L<sup>-1</sup> (n = 43), respectively. The concentrations of Fe<sup>2+</sup> varied from 1.1 mg·L<sup>-1</sup> in December of 2005 to 12.5 mg·L<sup>-1</sup> in December of 2004, whereas of Fe<sup>3+</sup> from 0 mg·L<sup>-1</sup> in December of 2005 to 13.0 mg·L<sup>-1</sup> in January of 2005 (mean values are presented in Table 1). The highest level of total Fe (24.0 mg·L<sup>-1</sup>) was recorded in January of 2005.

It should be stressed that at end July of 2004 at the foot of the western wall several separated pink to dark-red puddles were noted. They quickly disappeared after a heavy rainfall. The pH of these puddles varied from 2.10 to 2.23, whereas conductivity was in the range of 1108–1347 μS·cm<sup>-1</sup>. There was a relationship between the pH and water color; the dark-red puddle revealed the lowest pH value (possibly as a result of the action of bacteria). Strangely enough, these puddles were inhabited by organisms resembling Tubifex worms. However, the most acidic dark-red puddles appeared at the same site on December 4 and 5, 2004. Their pH varied from 1.52 to 1.60, and conductivity from 10.07 to 14.30 mS·cm<sup>-1</sup>. Moreover, these puddles contained distinctly raised concentrations of SO<sub>4</sub><sup>2-</sup> (7.75 g·L<sup>-1</sup>) and Fe total (1.26 g·L<sup>-1</sup>), including Fe<sup>2+</sup> (0.98 g·L<sup>-1</sup>).

The chemical composition of pyrite, sediment and carbonaceous clayey shales is highlighted by an increased

amount of arsenic, reaching 0.97%, 0.15% and 0.11%, respectively (Table 4). The high concentrations of arsenic (up to 6.5%) in some parts of pyrite grains were also recorded by an EDS ISIS Detector (Fig. 4D). Moreover, the pyrite examined is enriched in Co (31 mg·kg<sup>-1</sup>), Cu (123 mg·kg<sup>-1</sup>) and Ni (186 mg·kg<sup>-1</sup>). The presence of these three elements was also confirmed by an EDS ISIS Detector.

The X-ray diffraction and SEM/EDS determinations indicate that pyrite is the only primary sulfide mineral present here; marcasite occurs in trace amounts as a secondary mineral in some of the goethite accumulations. The pyrite consists of an-, sub- and euhedral (cubic) grains commonly varying from 0.0X to 0.2 mm in diameter (Fig. 3A – D). The SEM images show distribution of arsenic in a pyrite groundmass (Fig. 4A – D). The arsenic-rich pyrite forms veinlets cutting arsenic-depleted pyrite aggregates, or more commonly alternating bands at the pyrite grain edges. The spatial distribution of As and Cu in pyrite grains is depicted in Figs. 4E and F. This indicates a periodic change in chemical composition of fluids during hydrothermal activity. Most of the pyrite accumulations are accompanied by fine- and medium-grained quartz and scarce clay minerals (kaolinite). Some of the fissures in pyrite grains are filled in by secondary quartz. Accessory minerals are represented by zircon ZrSiO<sub>4</sub> and probably xenotime Y[PO<sub>4</sub>] (Figs. 5A and B), as well as by rutile

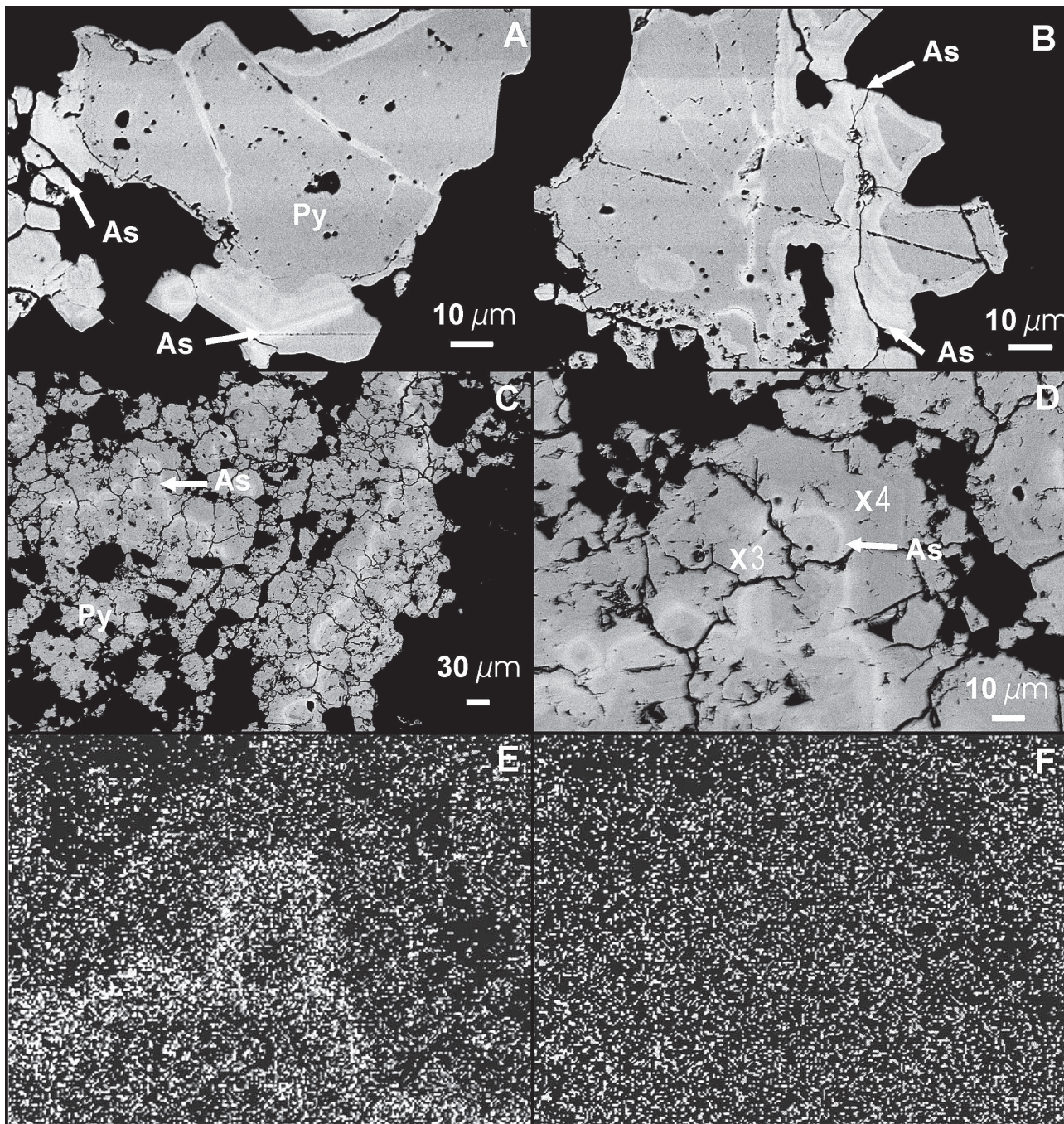


Fig. 4. SEM images. (A) Light gray As-rich pyrite forming veinlets and alternating bands with darker As-depleted pyrite. (B) Microbreccia composed of As-depleted pyrite grains coated with banded As-rich pyrite. Various shades of color reflect variations in the As content. (C) (D) As-rich pyrite bands in a coarser-grained As-depleted pyrite aggregate. Microanalysis for point 3: As – 6.5%, Co, Cu and Ni in trace amounts, and for point 4: As – 2.0%, Cu and Ni in trace amounts. (E) (F) EDS elemental maps for As and Cu in sample (D). The spatial distribution pattern of As coincides with light gray As-rich pyrite bands. In contrast, Cu is evenly distributed in pyrite grains.

TiO<sub>2</sub>. Most of the zircon grains show a zonal microstructure (Fig. 5B).

Hematite grains cemented by goethite occur in the quartzite of the northern part of the section, which is also highlighted by lack of any significant pyrite accumulations (Fig. 5C). In contrast, the goethite of the central section forms geode-like accumulations (Fig. 5D). These accumulations are a product of pyrite weathering. It is

interesting to note that goethite also contains As and Ni (Fig. 5E and F). The SEM images coupled with BEI technique did not record any sulfide mineral inclusions (larger than 3 nm in diameter) in the pyrite groundmass. Lack of As-minerals and zonal distribution of As (Figs. 4E and 5E) may indicate that arsenic replaces both sulfur and iron in FeS<sub>2</sub>, not only sulfur as indicated by Kolker and Nordstrom [30].

Except for arsenic, the water sediment and carbonaceous clayey shales are highlighted by an increased amount of Al, Ba, Cr, Fe, Si, Ti and V. The bentonite and related soil show high concentrations of Al, Cr, Si, Ti and V; the former reveals only trace amounts of As (Table 4). The mineral composition of water sediment, shale, bentonite and soil does not markedly differ: quartz, clay minerals (kaolinite, illite), muscovite are prevalent while feldspar (in bentonite) and alunite (in soil) are scarce; no barite was noted in the media examined.

The saturation indices show that goethite and hematite tend to precipitate from solution to sediments (high SI values), while quartz (SI = -0.17 to 0.05) generally remain in a state of equilibrium. The other selected minerals, especially chlorite, would dissolve due to the negative SI values (Table 5).

### Discussion

There are dozens of major geogenic and/or anthropogenic sources that can account for pollution of natural waters. One of the most important pollution sources is the oxidation of pyrite, causing acidity and triggering remobilization of heavy metals [e.g. 28, 31]. Acid precipitation is another common cause of low pH in some natural waters of vast areas, affecting aqueous organisms [e.g. 32]. However, this is not the case in the study area, as evidenced by the chemistry of a small pond from the pit verge. This water

reveals higher pH similar to that of unpolluted rainwater, very low conductivity and concentrations of ions, especially  $\text{SO}_4^{2-}$ . The pH is controlled by a variable amount of dissolved atmospheric and biogenic  $\text{CO}_2$ , and humic and fulvic acids produced through decay of aquatic plants.

In contrast, the pit pond water shows a lower pH, and higher conductivity and concentrations of ions, especially metals and sulfate (table 3). Seasonal variations in the pH of the acidic pit water may be linked to different physicochemical and biological factors, *i.e.* dilution, evaporation, reduction of sulfate, oxidation of  $\text{Fe}^{2+}$ , hydrolysis of  $\text{Fe}_2(\text{SO}_4)_3$ , water and air temperatures, variable bacterial activity, combined with flushing effects resulting from occasional influx of highly acidic water from the exposed pyritiferous zone.

The comparative chemical and mineralogical determinations performed on different media indicate that the weathering of pyrite is a principal source of most heavy metals (As, Cd, Co, Cr, Cu, Fe, Ni, Zn) and sulfate in water. The remaining cations (Al, Ca, K, Na, Si, Sr, V) have been derived from primary and secondary aluminosilicates making up clayey shales and pyroclastic rocks. Mn appears to be associated with clayey shales, and pyroclastic rocks.

Due to its large surface area available for attack by weathering agents, micro- and fine-grained pyrite tends to oxidize much more rapidly than its coarser equivalents. In the study area, white-to-pale green coatings (melanterite and other related species) and dark-gray pyritiferous mud

Table 5. Saturation indices for identified minerals calculated with PHREEQC program for Windows [22].

Phase	Water sampling points (sampling date)			
	1 (May 2004)	2 (May 2004)	3 (May 2004)	3 (Sept. 2004)
Alunite	-4.93	-4.99	-4.93	-4.33
Ca-montmorillonite	-12.37	-12.44	-12.47	-11.85
Chalcedony	-0.56	-0.56	-0.57	-0.36
$\text{Fe}(\text{OH})_3$ (amorphous)	-1.89	-1.94	-1.89	-1.57
Chlorite (14Å)	-63.98	-64.14	-64.07	-63.47
Goethite	4.00	3.95	4.00	4.32
Hematite	10.00	9.91	10.00	10.64
Illite	-16.79	-16.87	-16.85	-16.15
K-feldspar	-11.66	-11.70	-11.65	-10.89
K-mica	-13.56	-13.65	-13.60	-13.00
Kaolinite	-6.96	-7.01	-7.03	-6.75
Melanterite	-5.10	-5.09	-5.09	-4.98
Quartz	-0.16	-0.16	-0.17	0.05
$\text{SiO}_2$ (amorphous)	-1.40	-1.40	-1.41	-1.20

NOTE: Saturation indices for samples 1 and 3 were calculated on the assumption that 70% of total Fe was in 2+ oxidation state. For location of sampling points see Fig. 1

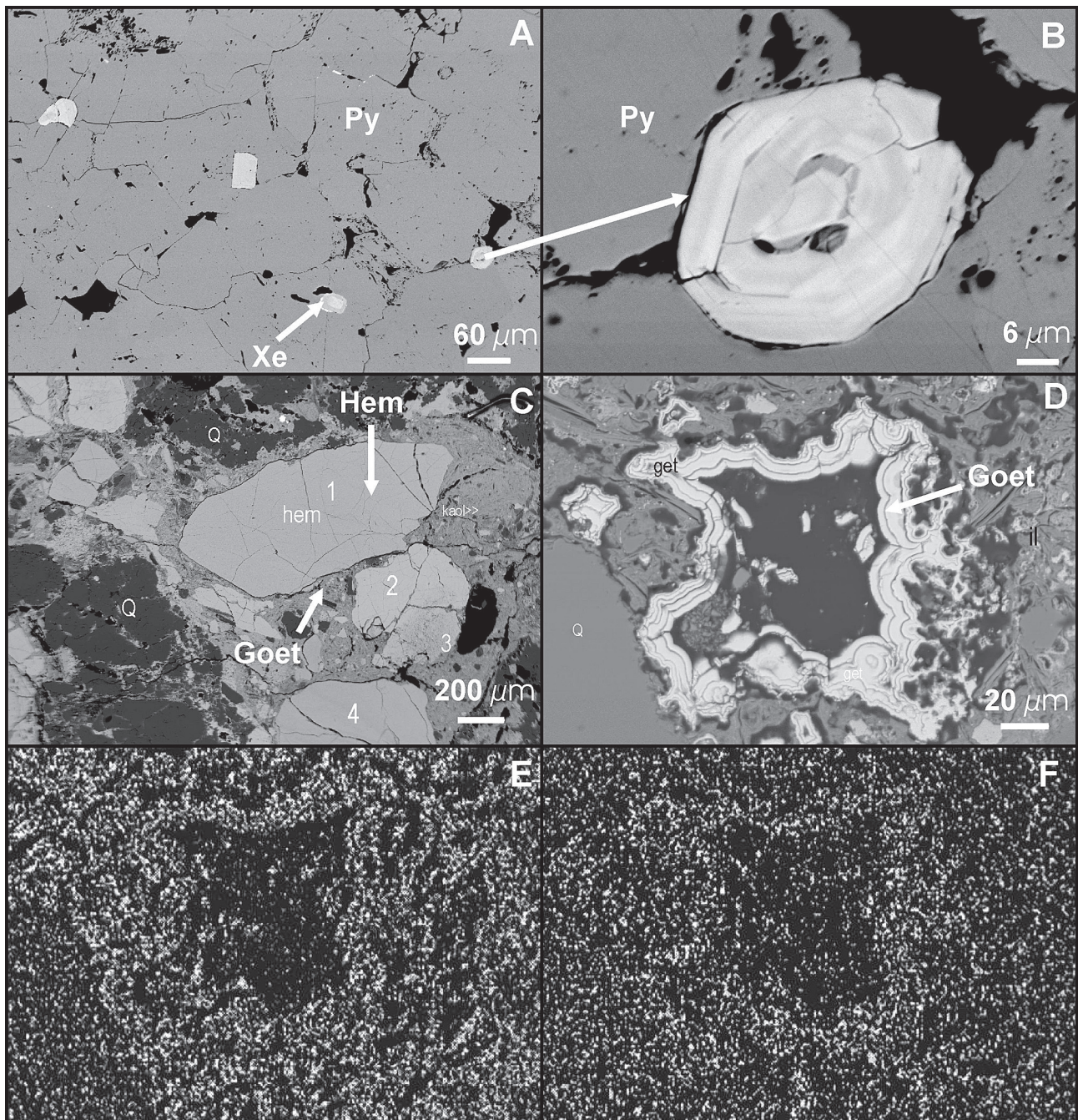


Fig. 5. (A) Pyrite aggregate with 4 sub- and euhedral zircon grains showing a zonal microstructure; the second to the right zircon grain exhibits a light gray rim of inferred xenotime (Xe). (B) The right zircon grain shows a zonal microstructure. (C) Microbreccia composed of hematite and quartz grains cemented by goethite. Scarce is kaolinite. (D) Alternating bands of goethite reflecting progressive growth toward the void. (E) (F) EDS elemental maps for As and Ni in sample (D). The spatial distribution pattern of this elements coincides with alternating bands of goethite.

covering surfaces of pyrite-quartz veinlets are often observed. Moreover, the investigations of pyrite and marcasite from different metal ore deposits indicate that arsenic-rich varieties weather (even without liquid water, merely from the reaction with water vapor in the air) more easily than their arsenic-free equivalents [33]. Another factor that may influence this process is the specific texture of the pyrite accumulations, *i.e.* the presence of alternating bands and

veinlets of the As-rich pyrite within the As-depleted pyrite. The concentrations of remaining trace elements, *e.g.* Ni, Cu, Co, Pb, Cd, in the pyrite examined are too low to play an important role in weathering of this mineral [33].

The reaction (5) (see Introduction section) produces a considerable amount of hydrogen ions, and seems to play a decisive role in developing additional acidity of water. A decrease in the pH to about 2.5–3.0 makes im-

possible further direct precipitation of Al, As, Co, Cr, Cu, Ni, Zn. However, these elements seem to be adsorbed by precipitated hydrous ferric oxides and hydroxides (and to a lesser extent by organic substance and clay minerals), which may be evidenced by distinctly raised concentrations of Fe (from 3.96% in May of 2004 to 6.88% in September of 2004), As (from 1067 to 1138 mg kg<sup>-1</sup>), Ba (from 877 to 1044 mg kg<sup>-1</sup>) and other trace metals in the sediment. An increase in the mean pH (from 2.61 to 3.13) and Fe<sup>3+</sup> levels (from 1.6 to 8.5 mg·L<sup>-1</sup>) may have provided conditions for coprecipitation and adsorption of these elements that had been dissolved in the acidic pit water [34]. Because hematite and goethite are also reportedly effective for arsenic adsorption [35], which is why hydrous ferric oxides and hydroxides can also play an important role in controlling the extremely low concentrations of heavy metals in the examined water. Moreover, the high sulfate/iron ratio (from 10 to 89), exceeding the theoretical ratio for pyrite (2), indicates iron deficiency in the water and precipitation according to oxidation-hydrolysis reactions (3, 5).

The field chemical determinations revealed variable concentrations of two iron species, *i.e.* Fe<sup>2+</sup> and Fe<sup>3+</sup>, in the pit water (Table 1). A mixture of ferrous and ferric ions in the water indicated bacterially induced oxidation, given that abiotic oxidation of Fe<sup>2+</sup> to Fe<sup>3+</sup> was strongly inhibited at pH <4, the dissolved iron remained in the ferrous state [36, 37]. The raised chemical oxygen demand (from 12.1 to 28.8 µg·L<sup>-1</sup>) may have been caused by a higher concentration of organic matter (Table 3). Ferrous iron concentrations were higher on sunny days, which may indicate that the amount of dissolved ferric iron and colloidal hydrous ferric oxides and hydroxides is reduced by solar radiation; however, it should be emphasized that the same effect may result from decreased activity of iron-oxidizing bacteria [*e.g.* 38-40]. The theoretical concentration of SO<sub>4</sub><sup>2-</sup> (mostly in the form of H<sub>2</sub>SO<sub>4</sub>), averaging 131 mg·L<sup>-1</sup>, is sufficient to keep the low acidity recorded in the water examined.

The extremely acidic and iron- and sulfate-rich puddles, which form near the central part of the western wall, indicate the direct source and pathway of acidic water. These puddles are washed away during heavy rainfalls mixing with the pit pond water. As a result of these inflows, the pH of the pit pond water decreases.

The uniqueness of this acidic pit water is highlighted by comparing its chemistry with that of surface waters from other localities of Poland (Sudetes, Upper Silesia) and worldwide (Tables 6 and 7). Except for three gravel pits from Kiiminki (Finland), which show higher pH, lower contents of Fe and SO<sub>4</sub><sup>2-</sup> (Table 7) and raised concentrations of Cd (1.54–5.29 µg·L<sup>-1</sup>), Mn (700–800 µg·L<sup>-1</sup>), Ni (100–230 µg·L<sup>-1</sup>) and Pb (120–170 µg·L<sup>-1</sup>) [41], no other sites reveal simultaneously such low pH, conductivity, and concentrations of sulfates and metals. This quality is especially highlighted when comparing the results of a field study performed in September 2004 in the Podwiśniówka locality and the “Purple Lake” in the Sudetes (Table 6). Acid mine waters of different localities worldwide are characterized by low pH, high metal (including iron and aluminum) and sulfate concentrations [2]. The water examined reflects only one of these parameters, *i.e.* pH. Both the low pH and low levels of sulfates and heavy metals in the Podwiśniówka pit pond water can be explained by the following combined factors: (i) presence of easily weathering micro- and fine-grained pyrite, (ii) occurrence of arsenic-rich pyrite in form of alternating bands and veinlets within arsenic-depleted pyrite, (iii) lack of other metal-supplying sulfides, (iv) lack of buffering gangue minerals and parent rocks (not acid-generating or acid-consuming), (v) bacterially induced decomposition of sulfate, and (vi) hydrolysis of dissolved Fe<sub>2</sub>(SO<sub>4</sub>)<sub>3</sub> and precipitation of colloidal hydrous ferric oxides and hydroxides that are highlighted by efficient adsorption of many elements.

## Conclusions

The following conclusions can be drawn from the data obtained:

1. The Podwiśniówka pit water is characterized by the distinctly low pH and low concentrations of sulfates and heavy metals compared to other acidic mine/rock waters from Poland, other European countries, and the U.S.A. These two combined parameters make the chemistry of this water unique.
2. The principal sulfide mineral is pyrite; marcasite occurs only in trace amounts. No sulfide inclusions larger

Table 6. Concentrations of SO<sub>4</sub><sup>2-</sup> and selected elements in the waters of the Podwiśniówka pit pond (Holy Cross Mountains) and “Purple Lake” with a tributary stream (Sudetes Mts, Poland).

Locality	SO <sub>4</sub> <sup>2-</sup> mg·L <sup>-1</sup>	Al	As	Cd	Cr	Cu	Fe	Mg	Mn	Ni	Zn
		µg·L <sup>-1</sup>									
Podwiśniówka*	150	4950	20	1	14	151	6250	2000	289	50	84
“Purple Lake” <sup>1</sup>	1486	44760	<12	4	70	1307	146700	89910	1527	201	277
Tributary stream <sup>1</sup>	474	11750	<12	2	<4	221	19080	29260	1169	71	101

NOTE: Pb – <10 mg·L<sup>-1</sup>. \*Geometric mean concentrations of 3 samples collected on May 25, 2004; <sup>1</sup>[20]

Table 7. Comparison of pH, conductivity and concentrations of  $\text{SO}_4^{2-}$  and Fe of surface waters from the Podwiśniówka pit pond and selected areas of Europe and U.S.A.

Location	pH	EC $\mu\text{S}\cdot\text{cm}^{-1}$	$\text{SO}_4^{2-}$	Fe total
			$\text{mg}\cdot\text{L}^{-1}$	
Podwiśniówka quarry (Holy Cross Mts)* <sup>a</sup>	2.59 – 2.65	508 – 686	149 – 151	6.1
Podwiśniówka quarry (Holy Cross Mts)* <sup>b</sup>	3.07 – 3.19	431 – 920	285	13.0
“Purple Lake” (Sudetes)* <sup>c</sup>	2.93 – 3.03	2600 – 3240	1375 – 1750	120 – 200
“Purple Lake” (Sudetes) <sup>1</sup>	2.5 – 2.8	1713 – 4720	892 – 2378	146.7
Niwka-Modrzejów coal mine (Upper Silesia) <sup>2</sup>	3.1	–	2660	–
As Pontes – streams type I (Galicia, NE Spain) <sup>3</sup>	2.2 – 3.5	1000 – 6500	4500 – 5000	700 – 1600
As Pontes – streams type IIIa (Galicia, NE Spain) (mean values) <sup>3</sup>	3.1 – 3.4	1670 – 2820	1082 – 2616	6.2 – 296.5
Gravel pit 14 on Jolosharju esker (Finland) <sup>4</sup>	3.6	–	84	0.9
Gravel pit 15 on Jolosharju esker (Finland) <sup>4</sup>	3.4	–	126	4.1
Gravel pit 17 on Jolosharju esker (Finland) <sup>4</sup>	3.6	–	88	1.0
Alum Creek (S Colorado, USA) <sup>5</sup>	2.64	1350	800	141
Bitter Creek (S. Colorado, USA) <sup>5</sup>	3.44	340	85	5.1
Missionary E Seep (Gamble Gulch, Colorado, USA) <sup>6</sup>	3.8	–	1540	150
Tip Top Adit (Gamble Gulch, Colorado, USA) <sup>6</sup>	3.8	–	300	4.7
Leviathan mine, Alpine County, California, USA <sup>7</sup>	3.25	–	483	18.4

\*Laboratory analyses: <sup>a</sup>May 25, 2004 (n = 4); <sup>b</sup>September 26, 2004 (n = 2); <sup>c</sup>September 17, 2004 (n = 5); <sup>1</sup>[20]; <sup>2</sup>[21]; <sup>3</sup>[42]; <sup>4</sup>[41]; <sup>5</sup>[43]; <sup>6</sup>[44]; <sup>7</sup>[45]

than 3 nm in diameter have been recorded. The pyrite is micro- to fine-grained, showing zonal distribution of arsenic. This element seems to replace both sulfur and iron in  $\text{FeS}_2$ .

- The study area is highlighted by lack of buffering gangue and rock-forming minerals. This is the main reason why the chemistry of the acidic pit water is greatly influenced by pyrite weathering mediated by complex chemical and microbiological reactions.
- The arsenic-rich pyrite is a source of raised concentrations of arsenic in the water sediment, which is of great concern for the environment.
- Except for somewhat elevated levels of arsenic and nickel, the water does not severely affect the environment.

### Acknowledgements

We are grateful to Irena Budzyk and Wanda Narkiewicz of the Central Chemical Laboratory of the Polish Geological Institute in Warsaw for performing XRF and XRD analyses. We also thank Dr. Richard Wanty of the U.S. Geological Survey for his assistance in PHREEQC modeling. This study was supported by a research grant from the Ministry of Science and Higher Education (No. 2 P04G 041 30).

### References

- NORDSTROM D.K., ALPERS C.N., BALL J.W. Measurement of negative pH and extremely high metal concentrations in acid mine water from Iron Mountain, California. *Geol. Soc. Am. Annual Meeting. Abstract and Programs* **23** (5), A.383, **1991**.
- NORDSTROM D.K., ALPERS C.N. Geochemistry of Acid Mine Waters. [In:] Plumlee G.S., Logsdon M.J. (eds.). *The Environmental Geochemistry of Mineral Deposits, Part A. Processes, Techniques, and Health Issues*. *Soc. Econ. Geologists. Rev. in Econ. Geology* **6A**, pp.133-160, **1999**.
- NORDSTROM D.K., ALPERS C.N., PTACEK C.J., BLOWERS D.W. Negative pH and Extremely Acid Mine Waters from Iron Mountain Superfund site, California. *Environ. Sci. Technol.* **34**(2), 254, **2000**.
- CHAPMAN M.M., JONES D.R., JUNG R.F. Processes controlling metal ion attenuation in acid mine drainage streams. *Geochim. Cosmochim. Acta* **47**, 1957, **1983**.
- KLEINMANN R.L.P. Acid mine drainage in the United States – Controlling the impact on streams and rivers. 4<sup>th</sup> World Congress on the Conservation of the Built and Natural Environments. University of Toronto, pp. 1-10, **1989**.
- FERRIS F.G., TAZAKI K., FYFE W.S. Iron oxides in acid mine drainage environments and their associated bacteria. *Chem. Geol.* **74**, 321, **1989**.

7. PRATT A.R., NESBITT H.W., MUIR I.J. Generation of acids from mine wastes: oxidative leaching of pyrrhotite in dilute H<sub>2</sub>SO<sub>4</sub> solutions at pH 3.0. *Geochim. Cosmochim. Acta* **58**, 5147, **1994**.
8. GOLDFARB R.J., NELSON S.W., TAYLOR C.D., D'ANGELO W.M., MEIER A.L. Acid-mine drainage associated with volcanogenic massive sulfide deposits, Prince William Sound, Alaska. [In:] Moore T.E., Dumoulin J.A. (eds.). *Geologic studies in Alaska by the U.S. Geological Survey*, 1994. U.S. Geol. Surv. Bull. **2152**, 3, **1996**.
9. GARRELS R.M., THOMPSON M.E. Oxidation of pyrite in ferric sulfate solution. *Am. J. Sci.* **258**, 57, **1960**.
10. WIERSMA C.L., RIMSTIDT J.D. Rates of reaction of pyrite and marcasite with ferric iron at pH 2. *Geochim. Cosmochim. Acta* **48**, 85, **1984**.
11. MCKIBBEN M.A., BARNES A.L. Oxidation of pyrite in low temperature acidic solutions: rate laws and surface textures. *Geochim. Cosmochim. Acta* **50**, 1509, **1986**.
12. MOSES C.O., NORDSTROM D.K., HERMAN J.S., MILLS A.L. Aqueous pyrite oxidation by dissolved oxygen and by ferric iron. *Geochim. Cosmochim. Acta* **51**, 1561, **1987**.
13. BLOWES D.W., AL. T., LORTIE L., GOULD W.D., JAMBOR J.L. Microbiological, chemical, and mineralogical characterization of the Kidd Creek mine tailings impoundment, Timmins area, Ontario. *Geomicrobiol. J.* **13**, 13, **1995**.
14. MILLS A.L. The Role of Bacteria in Environmental Geochemistry. [In:] Filipek L.H., Plumlee G.S. (eds.). *The Environmental Geochemistry of Mineral Deposits, Part A. Processes, Techniques, and Health Issues. Soc. Econ. Geologists. Rev. in Econ. Geology* **6B**, pp. 125-132, **1999**.
15. NORDSTROM D.K., SOUTHAM G. Geomicrobiology of sulfide mineral oxidation. [In:] Banfield J.F., Nealon K.H. (eds.). *Geomicrobiology – Interactions between Microbes and Minerals: Reviews in Mineralogy. Miner. Soc. Am., Washington, D.C.* **35**, pp. 361-390, **1997**.
16. BLOWES D.W., PTACEK C.J., JAMBOR J.L. Remediation and prevention of low-quality from tailings impoundments. [In:] Jambor J.L., Blowes D.W. (eds.). *The Environmental Geochemistry of Sulfide Mine-Wastes, Miner. Assoc. Canada, Short Course Notes* **22**, pp. 365-379, **1994**.
17. EVANGELOU V.P. Pyrite oxidation and its control. CRC Press, Boca Raton, Fla., **1995**.
18. PLUMLEE G.S., LOGSDON M.J. An Earth-System Science Toolkit for Environmentally Friendly Mineral Resource Development. [In:] Plumlee G.S., Logsdon M.J. (eds.). *The Environmental Geochemistry of Mineral Deposits, Part A. Processes, Techniques, and Health Issues. Soc. of Econ. Geologists. Rev. in Econ. Geology* **6A**, pp. 1-27, **1999**.
19. MALMSTRÖM M.E., GLEISNER M., HERBERT R.B. Element discharge from pyritic mine tailings at limited oxygen availability in column experiments. *Appl. Geochem.* **21**, 184, **2006**.
20. JEZIERSKI P. Chemistry of groundwaters and their dynamics in the Rudawy Janowickie area (Sudetes). Doctor's Thesis. Institute of Geological Sciences, University of Wrocław **2002** [In Polish].
21. PLUTA I., HAŁAS S. Identification of mine waters from the Powstańców Śląskich and Niwka-Modrzejów Coal Mines of the Upper Silesian Coal Basin by <sup>34</sup>S and <sup>18</sup>O in sulphates. 8<sup>th</sup> Intern. Conf. Hydrogeochemia, June 24-25, Ostrava, Czech Republic, pp. 97, **2004**.
22. PARKHURST D.L., APELLO C.A.J. User's guide to PHREEQC (version 2) – a computer program for speciation, batch-reaction, one-dimensional transport, and inverse geochemical calculations. U.S. Geol. Surv. Water-Resources Investigations Report **99-4259**, pp. 312, **1999**.
23. WANTY R.B., MILLER W.R., BRIGGS P.H., McHUGH J.B. Geochemical Processes Controlling Uranium Mobility in Mine Drainages. [In:] Plumlee G.S., Logsdon M.J. (eds.). *The Environmental Geochemistry of Mineral Deposits, Part A. Processes, Techniques, and Health Issues. Soc. of Econ. Geologists. Rev. in Econ. Geology* **6A**, pp. 201-213, **1999**.
24. ORŁOWSKI S. Stratigraphy of the Cambrian System in the Holy Cross Mts. *Geol. Quart.* **32**, 525, **1988**.
25. MIZERSKI W. Geotectonic evolution of the Holy Cross Mts in Central Europe. *Biul. Państw. Inst. Geol. (Pol. Geol. Inst. Bull.)* **327**, 1, **1995**.
26. MIZERSKI W. Holy Cross Mountains in the Caledonian, Variscan and Alpine cycles – major problems, open questions. *Prz. Geol. (Pol. Geol. Rev.)* **52** (8/2), 774, **2004**.
27. KOWALCZEWSKI Z., DADLEZ R. Tectonics of the Cambrian in the Wiśniówka area (Holy Cross Mts, central Poland). *Geol. Quart.* **40**, 23, **1996**.
28. PLUMLEE G.S., SMITH K.S., MONTOUR M.R., FICKLIN W.H., MOSIER E.L. Geologic Controls on the Composition of Natural Waters and Mine Waters Draining Diverse Mineral-Deposits Types. [In:] Filipek L.H., Plumlee G.S. (eds.). *The Environmental Geochemistry of Mineral Deposits, Part A. Processes, Techniques, and Health Issues. Soc. Econ. Geologists. Rev. in Econ. Geology* **6B**, pp. 373-407, **1999**.
29. TARVAINEN T., SALMINEN R. FOREGS Geochemical Mapping Field and Laboratory Manual. *Geologian tutkimuskeskus* **XX**, 1, **1997**.
30. KOLKER A., NORDSTROM D.K. Occurrence and micro-distribution of arsenic in pyrite. U.S. Geol. Surv. website (<http://wwwbr.cr.usgs.gov/Arsenic/>) **2001**.
31. RUNNELLS D.D., SHEPARD T.A., ANGINO E.E. Metals in water – Determining natural background concentrations in mineralized areas. *Environ. Sci. Technol.* **26**, 2316, **1992**.
32. HARRIMAN R., BATTARBEE R.W., MONTEITH D.T. Effects of acidic deposition on aquatic ecosystems. [In:] Bell J.N.B., Treshow M. (eds.). *Air Pollution and Plant Life. John Wiley and Sons, Chichester*, pp. 295-308, **2002**.
33. PLUMLEE G.S. The Environmental Geology of Mineral Deposits. [In:] Plumlee G.S., Logsdon M.J. (eds.). *The Environmental Geochemistry of Mineral Deposits, Part A. Processes, Techniques, and Health Issues. Soc. Econ. Geologists. Rev. in Econ. Geology* **6A**, pp. 71-116, **1999**.
34. SCHEMEL L.E., KIMBALL B.A., BENCALA K.E. Colloid formation and metal transport through two mixing zones affected by acid mine drainage near Silverton, Colorado. *Appl. Geochem.* **15**, 1003, **2000**.
35. ZHANG W., SINGH P., PALING E., DELIDES S. Arsenic removal from contaminated water by natural iron ores. *Min. Eng.* **17**, 517, **2004**.

36. LOWSON R.T. Aqueous oxidation of pyrite by molecular oxygen. *Chem. Rev.* **82**, 461, **1982**.
37. FICKLIN W.H., MOSIER E.L. Field Methods for Sampling and Analysis of Environmental Samples for Unstable and Selected Stable Constituents. [In:] Plumlee G.S., Logsdon M.J. (eds.). *The Environmental Geochemistry of Mineral Deposits, Part A. Processes, Techniques, and Health Issues.* Soc. Econ. Geologists. Rev. in *Econ. Geology* **6A**, pp. 249-264, 1999.
38. LE ROUX N.W., MARSHALL V.M. Effect of light on *Thiobacilli*. [In:] Schwartz W. (ed.). *Conference Bacterial Leaching, 1977.* GBF, Verlag Chemie, Weinheim, pp. 21-35 **1977**.
39. WAITE T.D., MOREL F.M.M. Photoreductive dissolution of colloidal iron oxides in natural waters. *Environ. Sci. Technol.* **18**, 860, **1984**.
40. MCKNIGHT D.M., KIMBALL B.A., BENCALA K.E. Iron photoreduction and oxidation in an acidic mountain stream. *Science* **240**, 637, **1988**.
41. PIISPANEN R., NYKYRI T. Acidification of groundwater in water-filled gravel pits – a new environmental and geomedical threat. *Environ. Geochem. Health.* **19** (3), 111, **1997**.
42. MONTERROSO C., MACÍAS F. Drainage waters affected by pyrite oxidation in a coal mine in Galicia (NW Spain): Composition and mineral stability. *Sci. Total Environ.* **216**, 121, **1998**.
43. MILLER W.R., MCHUGH J.B. Calculations of Geochemical Baselines of Stream Waters in the Vicinity of Summitville, Colorado, Before Historic Underground Mining and Prior to Recent Open-Pit Mining. [In:] Filipek L.H., Plumlee G.S. (eds.). *The Environmental Geochemistry of Mineral Deposits, Part A. Processes, Techniques, and Health Issues.* Soc. Econ. Geologists. Rev. in *Econ. Geology* **6B**, pp. 505-514. **1999**.
44. SMITH K.S. Metal Sorption on Mineral Surfaces: An Overview with Examples Relating to Mineral Deposits. [In:] Plumlee G.S., Logsdon M.J. (eds.). *The Environmental Geochemistry of Mineral Deposits, Part A. Processes, Techniques, and Health Issues.* Soc. Econ. Geologists. Rev. in *Econ. Geology* **6A**, pp. 125–132. **1999**.
45. BALL J.W., NORDSTROM D.K. Final revised analyses of major and trace elements from acid mine waters in the Leviathan mine drainage basin, California and Nevada – October 1981 to October 1982. U.S. Geol. Surv. Water-Resources Investigations Report. **89-4138**, pp. 151, **1989**.